Hindawi Publishing Corporation
International Journal of Polymer Science
Volume 2015, Article ID 863057, 13 pages
http://dx.doi.org/10.1155/2015/863057

Research Article

Shear Strength of Unreinforced Masonry Wall Retrofitted with Fiber Reinforced Polymer and Hybrid Sheet

Yun-Cheul Choi,[1] Hyun-Ki Choi,[2] Dongkeun Lee,[3] and Chang Sik Choi[4]

[1] *Department of Building Equipment and Fire Protection System, Chungwoon University, Chungnam 350-701, Republic of Korea*
[2] *Department of Fire and Disaster Prevention Engineering, Kyungnam University, Gyeongsangnam-do 631-701, Republic of Korea*
[3] *Department of Civil Engineering, Antalya International University, 07190 Antalya, Turkey*
[4] *Department of Architectural Engineering, Hanyang University, Seoul 133-791, Republic of Korea*

Correspondence should be addressed to Dongkeun Lee; dongkeun.lee@antalya.edu.tr

Received 14 June 2015; Revised 14 September 2015; Accepted 16 September 2015

Academic Editor: Gonzalo Martínez-Barrera

Unreinforced masonry (URM) structures represent a significant portion of existing historical structures around the world. Recent earthquakes have shown the need for seismic retrofitting for URM structures. Various types of strengthening methods have been used for URM structures. In particular, a strengthening technique using externally bonded (EB) fiber reinforced polymer (FRP) composites has attracted engineers since EB FRP materials effectively enhance the shear strength of URM walls with negligible change to cross-sectional area and weight of the walls. Research has been extensively conducted to determine characteristics of URM walls strengthened with EB FRP materials. However, it is still difficult to determine an appropriate retrofitting level due to the complexity of mechanical behavior of strengthened URM walls. In this study, in-plane behavior under lateral loading was, therefore, investigated on a full-scale nonstrengthened URM wall and URM walls retrofitted with two different FRP materials: carbon (CFRP) and hybrid (HFRP) sheets. The test results indicated that both FRP composites were effective in increasing shear strength in comparison with the control specimen. However, better performance was obtained with HFRP compared to CFRP. In addition, an equation for estimating effective strain was proposed, and the theoretical results were in good agreement with the experimental ones.

1. Introduction

In general, masonry structures are considered to be optimal for low-rise structures in many countries due to easy and fast construction, abundant material, and no special technique for construction. Although masonry structures are strong enough to resist large compressive stress, these structures have poor ductility and thus are vulnerable under dynamic loading such as earthquake. For instance, unreinforced masonry (URM) structures have been prohibited for public structures including schools since the Long Beach earthquake, of 1993, in California, USA. Even though structures were constructed to meet the high level seismic requirements of New Zealand, many of those were severely damaged and collapsed due to consecutive earthquakes, in 2010 and 2011. This resulted in a great deal of humans and property losses [1–3].

Recently, the risk of earthquake events has increased in many countries that have a low probability of earthquake occurrences. For example, the number of earthquakes in South Korea increased by 54.3% in the recent three years. As with many countries, there are many masonry structures constructed without meeting current seismic requirements and strengthening, especially in South Korea where there is even an obvious probability of earthquake. More specifically, low-rise masonry structures in South Korea are 30% of all domestic structures, over 40% of all domestic houses, and substantially vulnerable to earthquake [3, 4].

Due to the aforementioned reasons, research on strengthening URM walls has been extremely conducted. FEMA 356 suggests design guidelines of URM walls to resist lateral force and evaluation of existing structures on the basis of existing research results. In addition, FEMA 356 [5] indicates how to assess structures with damage or loss of capacity for strengthening and suggests various methods such as shotcrete, coating, reinforced core, and prestressed core for URM walls.

In particular, research on URM walls retrofitted with externally bonded (EB) fiber reinforced polymer (FRP) composite materials has been substantially conducted due to the well-known advantages of FRP materials (i.e., good corrosion resistance, light weight, ease of installation, and high specific stiffness and strength). In terms of the material properties of FRP composites, substantial research has been conducted. For instance, research on the effect of temperature has been carried out [6–10]. One of the serious issues on temperature is glass transition temperature (T_g). T_g of resin generally varies from 60 to 82°C. T_g of glass fiber, carbon fiber, and aramid fiber is 275, 1000, and 175°C, respectively. The mechanical properties of polymer adhesives are significantly reduced when the temperature is close to T_g. The time-dependent behavior of FRP composites is also a vital issue. It was reported that creep and relaxation of carbon fiber are practically zero [11]. Research has been also conducted to know the fatigue behavior of FRP composites [12, 13]. Sun and Chan [13] reported that the fatigue life of FRP composites was extended by increasing load frequency. From the standpoint of compressive behavior, the compressive strength of FRP composites is generally lower than tensile strength. For example, 78, 55, and 20% of the tensile strengths of carbon FRP (CFRP), glass FRP (GFRP), and aramid FRP (AFRP) were reported as the compressive strengths, respectively [14].

In addition to research at the material level, the structural behavior of URM walls strengthened with FRP composites has been considerably investigated. The common failure modes of URM walls strengthened in shear are the debonding of EB FRP composites, the rupture of FRP composites, or the failure of URM wall. In many tests, the debonding of EB FRP composites was observed [15–17]. It was reported that thicker and stiffer FRP composites were more susceptible to debonding. EB FRP sheets are prone to buckling under compression stress, causing debonding failure. This buckling of EB FRP sheets occurred during the tests [15]. The shear performance of URM walls strengthened with CFRP laminates was investigated [18]. It was reported that both strength and displacement were improved by using CFRP laminates. Research on the behavior of damaged URM walls strengthened with CFRP laminates was carried out by Gergely and Young [19]. ElGawady et al. [20] carried out experimental studies on shear strength of URM walls strengthened with FRP composites such as GFRP and AFRP composites. They suggested a model to predict shear strength of URM walls retrofitted with FRP composites. ElGawady et al. [21] recommended full surface cover strengthening for predamaged masonry walls rather than X-type configuration. They also reported that the walls strengthened with FRP sheets in the X-type configuration were affected by the existing cracks in the predamaged walls. Two different types of FRP material (CFRP versus GFRP) were compared [17]. They found that GFRP laminates were superior to CFRP laminates when it comes to shear capacity. The in-plane behavior of URM walls strengthened with a GFRP reinforced mortar coating was investigated [22]. Various mortars were used for the coating. It was reported that both strength and ductility were considerably increased. Two composite materials, ferrocement and GFRP, were used to strengthen confined masonry walls under vertical and lateral cyclic loading [23]. The wall specimens were retrofitted with three different FRP configurations of X-type, corner, and full coverage. It was found that the two composites were effective in improving the ductility and energy absorption significantly. However, lateral drift was slightly improved. Eight specimens were examined to investigate the in-plane behavior of URM walls strengthened with basalt FRP (BFRP) composites [24]. They reported that the failure mode of strengthened walls was different by using BFRP composites in comparison with the control wall. Furthermore, a design model for URM walls strengthened with BFRP composites was proposed in the study.

Although EB FRP composites do not reach their ultimate states, structures can fail by the debonding of composites from concrete substrate due to shear or flexural palling at the end of composite materials. Similarly, the deformation of composites is caused after concrete substrate deforms since EB FRP composites are bonded to the substrate, which is called passive strengthening technique [25]. Although there are various bonding methods to improve bond capacity between composites and concrete substrate in terms of the passive strengthening technique, methods using epoxy or polyester resins are generally used. In this study, epoxy resin was used. As mentioned previously, when epoxy is used, special care should be taken for the change of mechanical characteristics due to temperature. Thermal characteristics of FRP composites are influenced by the T_g of epoxy rather than that of fiber. It was reported that the spalling area of matrix increased and the mechanical properties of matrix decreased under high temperature such as 130°C. However, the tensile strength and stiffness of matrix tended to increase under low temperature such as −40°C due to the shrinkage of matrix [6–8, 26, 27]. Therefore, temperature can be an essential factor with respect to T_g. However, the effect of the environment on FRP composites is out of the scope of this study on the basis of the following reasons. Firstly, there are few factors influencing the mechanical properties of materials in the civil engineering environment excluding fire in comparison with aerospace and defense industry. Secondly, it is rare that FRP reinforcement under tensile stress will fail prior to the failure of masonry substrate since the tensile capacity of FRP reinforcement is generally superior to that of the substrate. Lastly, the URM walls examined in this study are interior curtain walls hardly affected by extraordinary environmental conditions. Therefore, it was assumed that FRP composites with epoxy resin were not affected by the environment in this study.

As mentioned above, considerable research has been conducted on URM walls strengthened with various FRP composites such as CFRP, GFRP, AFRP, and BFRP composites. However, research on the in-plane behavior of URM walls retrofitted with hybrid FRP (HFRP) is significantly limited. Therefore, the objective of this study is to investigate the in-plane behavior of URM walls strengthened with CFRP

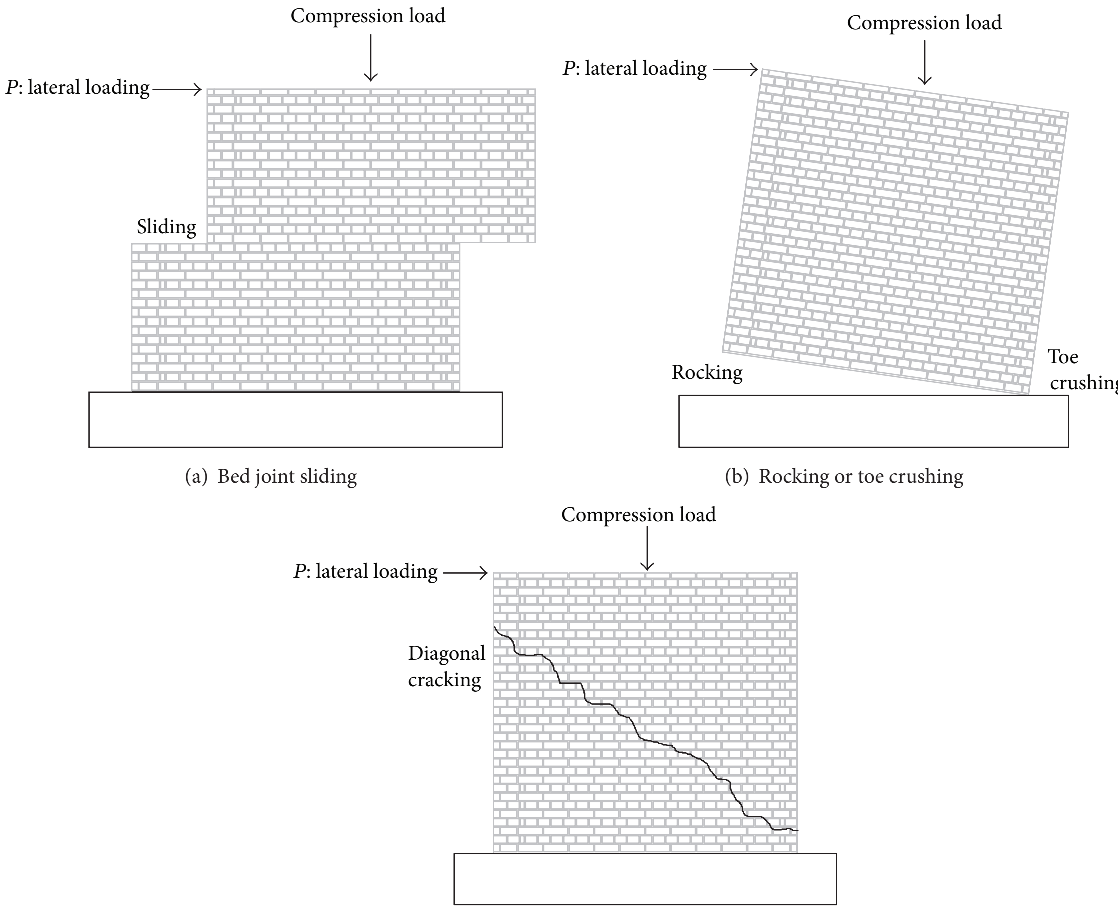

(a) Bed joint sliding

(b) Rocking or toe crushing

(c) Diagonal tension

Figure 1: Failure mode of unreinforced masonry wall.

and HFRP (GFRP plus AFRP) sheets under cyclic loading. Furthermore, an equation is proposed to estimate accurate effective strain and thus the shear strength of URM walls retrofitted with EB FRP composite materials.

2. Performance Appraisal of Nonreinforced and Reinforced Masonry Walls

Behavior of URM walls is quite different from that of reinforced masonry walls. In particular, failure modes of URM walls are substantially crucial since strengthening material FRP sheets have their own directional natures. Moreover, it is essential to know the strength of existing URM walls for determining the proper strengthening level. Thus, failure modes of URM walls have been divided into four categories in this study. Strength capacity of URM walls in each category was estimated in accordance with FEMA 356 [5].

2.1. Failure Mode and Related Strength of URM Walls. Failure modes of URM walls can be divided into shear and flexure categories, and then each category can be subdivided into deformation and force controlled actions. Failure modes can be determined depending on the length-to-height ratio (L/h) and the amount of compressive stress. Failure modes are summarized in Figure 1 and Table 1.

Table 1: Failure mode of unreinforced masonry wall by aspect ratio.

	Deformation controlled action	Force controlled action
$L/h < 1.0$	Rocking	Toe crushing
$L/h > 1.5$	Bed joint sliding	Diagonal tension

Shear strength of URM walls can be predicted using the estimation equations by FEMA 356 [5] as follows:

$$
\begin{gathered}
Q_{\mathrm{CE}} = V_{\mathrm{bjs}} = v_{\mathrm{me}} A_n, \\
Q_{\mathrm{CE}} = V_r = 0.9 \alpha P_E \left(\frac{L}{h_{\mathrm{eff}}} \right), \\
Q_{\mathrm{CE}} = V_{\mathrm{tc}} = \alpha P_E \left(\frac{L}{h_{\mathrm{eff}}} \right) \left(1 - \frac{f_a}{0.7 f'_m} \right), \\
Q_{\mathrm{CE}} = V_{\mathrm{dt}} = f_{\mathrm{dt}} A_n \left(\frac{L}{h_{\mathrm{eff}}} \right) \left(1 + \frac{f_a}{f_{\mathrm{dt}}} \right),
\end{gathered}
\tag{1}
$$

where Q_{CE} is shear strength of URM wall, V_{bjs}, V_r, V_{tc}, and V_{dt} are shear strength in case of bed joint sliding, rocking, toe crushing, and diagonal tension, respectively, v_{me} is shear stress in case of bed joint sliding, A_n is bonding area of mortar, L is wall length, h_{eff} is wall height, α is boundary condition constant (0.5 and 1.0 for cantilever and both fixed ends, resp.), P_E is expected axial compressive force on wall, f_a is axial compressive stress (axial compressive force/area of wall), f'_m is compressive strength of masonry, and f_{dt} is diagonal tension stress.

2.2. Strength of URM Walls Retrofitted with FRP Sheet. Studies were conducted to predict the shear strength of URM walls strengthened with FRP composite materials. For instance, ElGawady [28] conducted research on the shear strength of URM walls retrofitted with FRP sheets using the shear strength estimation model suggested by Triantafillou [29]. The model by Triantafillou was derived to predict the shear strength of reinforced concrete (RC) beams strengthened with FRP sheets. In the model, the effective strain of the FRP sheet was used instead of ultimate strain as follows:

$$P = F_m + F_{\mathrm{FRP}},$$
$$F_{\mathrm{FRP}} = \rho_h E_{\mathrm{FRP}} \varepsilon_{\mathrm{eff}} t L, \tag{2}$$
$$\rho_h = \frac{A_{\mathrm{FRP}}}{Lt},$$

where F_m is strength of URM walls, F_{FRP} is effective strength of FRP material, ρ_h is strengthening ratio in horizontal direction, E_{FRP} is elastic modulus of FRP, $\varepsilon_{\mathrm{eff}}$ is effective strain of FRP, t is wall thickness, L is wall length, and A_{FRP} is cross-sectional area of FRP. Effective strain of the FRP sheet was derived using existing experimental data and is expressed as follows:

$$\varepsilon_{\mathrm{eff}} = \begin{cases} 0.0119 - 0.0205\left(\rho_h E_{\mathrm{FRP}}\right) + 0.0104\left(\rho_h E_{\mathrm{FRP}}\right)^2 & \text{when } 0 \le \rho_h E_{\mathrm{FRP}} \le 1\text{ GPa} \\ 0.0024 - 0.00065\left(\rho_h E_{\mathrm{FRP}}\right) & \text{when } \rho_h E_{\mathrm{FRP}} \ge 1\text{ GPa}. \end{cases} \tag{3}$$

AC 125 [30] model is the guideline suggested by the International Code Council (ICC). In accordance with AC 125 [30], lateral resistance of the FRP sheet applied to one side of URM or RC walls can be estimated using the following equations:

$$F_{\mathrm{FRP}} = 0.75\rho_h f_j t L,$$
$$f_j = 0.004 E_{\mathrm{FRP}} < 0.75 f_{\mathrm{FRP},u}, \tag{4}$$

where $f_{\mathrm{FRP},u}$ is ultimate tensile strength of FRP sheet and f_j is axial force of FRP sheet.

3. Specimens and Test Plan

In this study, the in-plane behavior of URM walls strengthened with unidirectional FRP sheet applied to one side of the walls was investigated to quantify the strengthening effectiveness of FRP composites. To achieve the purpose, three full-scale specimens were designed. One (URM-0.92) was nonstrengthened to serve as a control specimen and the other two (RTM-CFS-SF and RTM-HBRD-SF) were strengthened with CFRP and HFRP sheets, respectively. The aspect ratio (L/h) of the specimens was designed to be close to 1 for expressing rocking phenomenon under low axial force.

3.1. Material Properties. As mentioned above, two types of FRP composites were used. One is CFRP, a widely used strengthening material, and the other is HFRP, newly developed. HFRP was made of GFRP and AFRP to introduce advantages of the two FRP composites. The mechanical properties of the CFRP and HFRP composites were obtained experimentally in the laboratory and are provided in Table 2. The values provided in Table 2 are the average values of the three specimens tested. The values are not rounded off. The HFRP composite shows higher ultimate strain but lower tensile strength and elastic modulus than the CFRP composite. Both FRP composites are expected to improve deformability of URM walls from the standpoint of the ultimate strain of the FRP composites as listed in Table 2. The stress-strain relationships of both FRP composites are depicted in Figure 2.

Since the masonry wall specimens were full scale, commercially available cement bricks with dimensions of 190 × 90 × 57 mm were used. Bed joints of 10 mm and 1.0 B thickness were chosen. The average compressive strength of the bricks was obtained as 15.7 MPa following the test method per KS F 4004 (Table 3) [31]. Ordinary mortar was applied and 1 : 1 ratio was used for mixing cement and sand. The average compressive strength of the mortar was recorded as 8.4 MPa using specimens with dimensions of 50 × 50 × 50 mm.

3.2. Strengthening URM Walls Using FRP Sheet. The parts between the walls and their bases were strengthened with FRP composites in the vertical direction to avoid early flexural failure due to low axial force and aspect ratio. The strengthening amount to resist flexure was determined following the sectional analysis used for RC walls as depicted in Figure 3. The bricks and FRP sheets were assumed to resist compressive and tensile stresses only, respectively. The compressive stress block was assumed in accordance with ACI 318 [32]. One layer of FRP sheet was applied to one side of each strengthened wall to quantify the shear strengthening effectiveness of an FRP sheet. The strengthening amount for

Table 2: Material properties of FRP and resin.

Type		W_{frp} [g/m^2]	f_t [MPa]	E [GPa]	ε [%]
GFPR sheet	#1	88.98	2709.01	159.47	1.69
	#2	96.45	2867.75	166.26	1.72
	#3	93.57	2838.24	169.27	1.68
Hybrid sheet	#1	139.89	2322.27	64.14	3.62
	#2	150.76	2490.39	76.24	3.27
	#3	144.35	2510.44	72.65	3.46
Resin[1]		Tensile strength (MPa)	Tensile modulus (GP)	Elongation at break [%]	Density (g/cm^3)
Epoxy		85	10.5	0.8	1.2

[1]The properties are not obtained from the laboratory but are provided by the manufacturer.

Table 3: Material properties of URM.

Compressive strength of cement brick [MPa]		Compressive strength of mortar [MPa]		Compressive strength of prism [MPa]	
#1	14.29	#1	7.54	#1	11.92
#2	15.94	#2	8.64	#2	12.77
#3	15.97	#3	9.02	#3	12.86

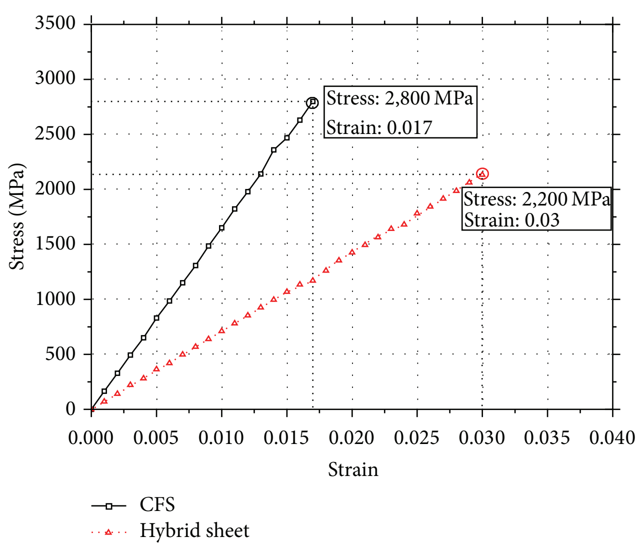

Figure 2: Stress-strain relationship of FRP sheet.

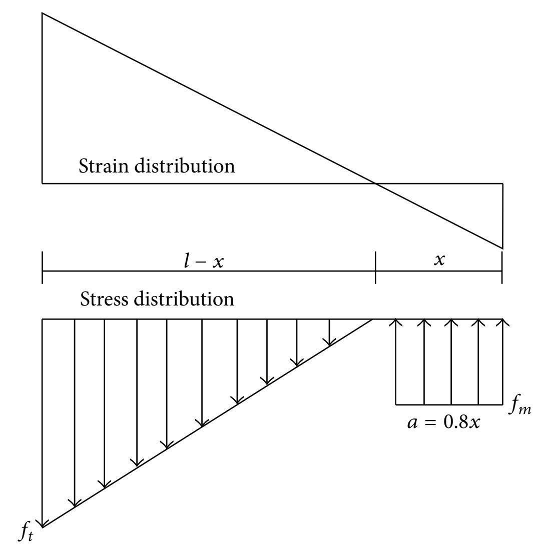

Figure 3: Flexural strength calculation of retrofitted specimen.

each strengthened specimen is listed in Table 4. The specimen dimensions and reinforcement details are illustrated in Figure 4.

3.3. Test Setup and Loading Protocol. As shown in Figure 5, the masonry wall specimens were manufactured on the precast RC base tied to the strong frame in the laboratory. A small compressive force was applied through the steel loading beam and self-weight of the masonry wall, since the masonry wall represented low-rise apartments. Lateral force was generated using a 1000 kN actuator attached to the steel loading beam on the top of the masonry wall specimen. As illustrated in Figure 5, the support frame was used to prevent the masonry wall from out-of-plane buckling.

The masonry wall specimens were tested using displacement control. Loading histories are depicted in Figure 6. The displacement control was based on the rotational angle of the specimens. In other words, a drift ratio of distance from the specimen bottom to the center of the actuator to lateral displacement increased from 0.1% with an increment of 0.1 (i.e., 0.1, 0.2, 0.3, 0.4, and 0.5%). Positive and negative cyclic loads were repeated three times per drift ratio.

4. Test Results

4.1. Failure Mode and Load-Displacement Relationship. Figure 7 shows crack patterns and failure modes of the tested specimens. The load-displacement relationships of the masonry wall specimens are depicted in Figure 8. The main test results are summarized in Table 5. Detailed test results of each specimen are as follows.

As a control specimen, URM-0.92 was a nonstrengthened masonry wall. After initial cracks formed, no additional load was transferred between the URM wall and base due to cracks

Table 4: List of specimens.

Specimen	H [mm]	L [mm]	Aspect ratio	t_{URM} [mm]	Retrofit material	t_{FRP} [mm]	FRP sheet layer	Brick element [mm]	Vertical reinforcement [mm]
URM-0.92									—
RTM-CFS-SF	2380	2400	0.92	190	CFRP	0.16	1	190 × 90 × 57	60
RTM-HBRD-SF					Hybrid	0.17	1		45

H: height of specimen, L: length of specimen, t_{URM}: URM thickness, and t_{FRP}: FRP thickness.

Table 5: Summary of test results.

Specimens		P_{cr} [kN]	P_y [kN]	P_{max} [kN]	δ_y [mm]	δ_{max} [mm]	$\delta_{failure}$ [mm]	θ_y [%]	θ_{max} [%]	μ	$P_{u,retrofit}/P_{max,URM}$
URM-0.92	Pos.	13	18	23	1.47	2.83	12.6	0.06	0.5	2.8	—
	Neg.	−5	−9	−12	−1.78	−9.8	−9.8	−0.08	−0.1	1.25	—
RTM-CFS-SF	Pos.	74	74	99	14.3	17.7	33.1	0.57	0.7	1.2	4.3
	Neg.	−54	−81	−108	−19	−28.1	−33	−0.94	−1.3	1.5	9
RTM-HBRD-SF	Pos.	63	104	139	17.6	32.8	43.4	0.65	1.3	1.8	6
	Neg.	−49	−90	−121	−22.6	−33.2	−43.3	−0.92	−1.4	1.5	1.2

All estimates associated with moment and shear computed based on actual material properties.
P_{cr}: initial crack load (measured), P_y: yield load by Park's method (measured), P_{max}: peak load (measured), δ_y: yield displacement (measured), δ_{max}: peak displacement (measured), $\delta_{failure}$: failure displacement (measured), θ_y: drift corresponding to the yielding, θ_{max}: drift corresponding to the yielding, u: ductility (δ_{max}/δ_y = deformation capacity), and $P_{u,retrofit}/P_{max,URM}$: strength increase ratio.

in the mortar between the URM wall and base, resulting in lifting of the URM wall with an ultimate load of 23 kN at a 0.2% drift ratio. After a 0.5% drift ratio, it was observed that displacement continuously increased without load increase due to the wall rotation. Thus, it appeared that, after the ultimate load was recorded, failure occurred due to the wall lifting at a drift ratio of 0.4%.

The specimen RTM-CFS-SF, strengthened with CFRP sheet, reached an ultimate load of 99 kN at a drift ratio of +0.69%. RTM-CFS-SF showed approximately 330% larger load-carrying capacity in comparison with URM-0.92. When the strengthened specimen reached the ultimate load, rupture of FRP sheet applied between the wall and base occurred with a loud sound. This was attributed to stress concentration at the debonding area of the FRP sheet from the wall. Then, the load-carrying capacity of the strengthened specimen rapidly decreased. After wall lifting was observed, failure of the FRP sheet propagated, and ultimately RTM-CFS-SF failed due to the crushing of the brick at the bottom of the masonry wall.

The other strengthened specimen with HFRP, RTM-HBRD-SF, presented an ultimate load of 139 kN at a drift ratio of +1.31%. RTM-HBRD-SF indicated approximately 504% and 40% larger load-carrying capacity than URM-0.92 and RTM-CFS-SF, respectively. In addition, unlike RTM-CFS-SF, RTM-HBRD-SF showed continuous load resistance capability and gradual decrease of load-carrying capacity after the ultimate load was reached. Due to the mechanical properties of HFRP (low modulus of elasticity and large ultimate strain), there was no rupture of the FRP sheet between the masonry wall and base. However, due to propagation of the diagonal crack following the mortar face, RTM-HBRD-SF failed with signs of HFRP sheet debonding from the masonry wall after a drift ratio of +1.5%.

4.2. Assessment of Deformability of FRP Sheet. To evaluate the contribution of the FRP sheet to shear strength improvement, strains were measured in the FRP sheets in the horizontal and vertical directions. Figure 9 depicts the strain distributions of the FRP sheets in the vertical direction of both strengthened specimens. Strain gages were attached on the locations of 400 and 750 mm from the wall side end and 200 mm from the connection line between the wall and base. The distance of 200 mm was chosen since the flexural crack of URM-0.92 formed at the same location. In the case of RTM-CFS-SF, it was found that a quite large stress concentration occurred at the bottom of the masonry wall at the ultimate. It seems that FRP sheets in the horizontal direction were not significantly effective in enhancing shear strength since the load-carrying capacity of RTM-CFS-SF suddenly dropped. On the contrary, strain distributions of RTM-HBRD-SF increased gradually and continuously, meaning that the FRP sheets in the horizontal direction substantially contributed to shear strength.

Figure 10 shows the strain distributions of FRP sheets in the horizontal direction of both strengthened specimens. Strain gages were attached on locations where critical cracks would most likely occur. In the case of RTM-CFS-SF, there was no additional strain increase after the ultimate. At the diagonal crack formation area, a strain of approximately 0.001 was measured. However, the strains of RTM-HBRD-SF continued to increase after the ultimate. A strain of

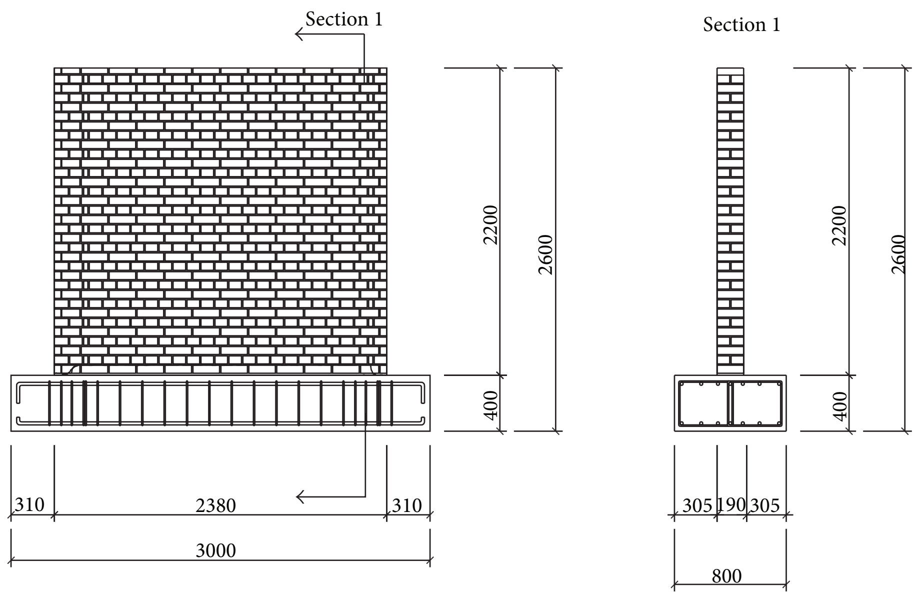

(a) URM-0.92

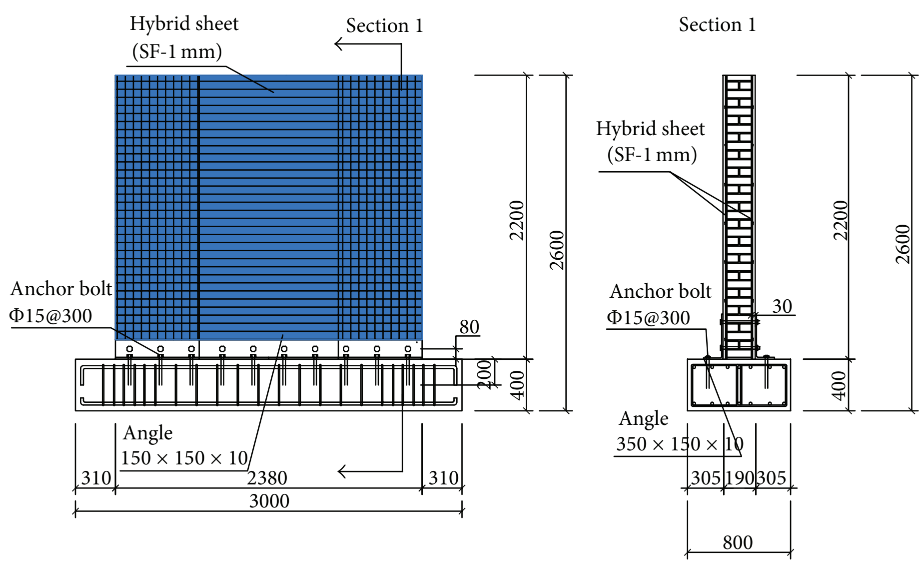

(b) Retrofitted specimen (RTM-CFS-SF, RTM-HBRD-SF)

Figure 4: Specimen dimensions (unit: mm).

approximately 0.003 was recorded at the diagonal crack formation area.

5. Appraisal of Shear Strengthening Capability of FRP Sheet

5.1. Evaluation of Shear Resistance through Strengthening. Figure 11 shows the shear strength comparison between theoretical and experimental results for RTM-CFS-SF and RTM-HBRD-SF. The theoretical values were obtained using the shear strength model suggested by Triantafillou [29]. The estimated values present a considerably large difference from the test results (523% and 311% for RTM-CFS-SF and RTM-HBRD-SF, resp.). This was attributed to the fact that the strain of the FRP sheet at the ultimate was fairly small in comparison with that of the shear strength model and the ultimate value.

5.2. Shear Strength Estimation through Nonlinear Regression Analysis. As stated before, the shear strength model by Triantafillou showed poor agreement with the test results. Effective strain was a critical factor of the shear strength model and obtained through nonlinear regression analysis on the basis of experimental data. In this study, a theoretical study was, therefore, conducted through nonlinear regression analysis to find a better effective strain and thus to estimate more accurate shear strength for a URM wall strengthened with FRP sheet.

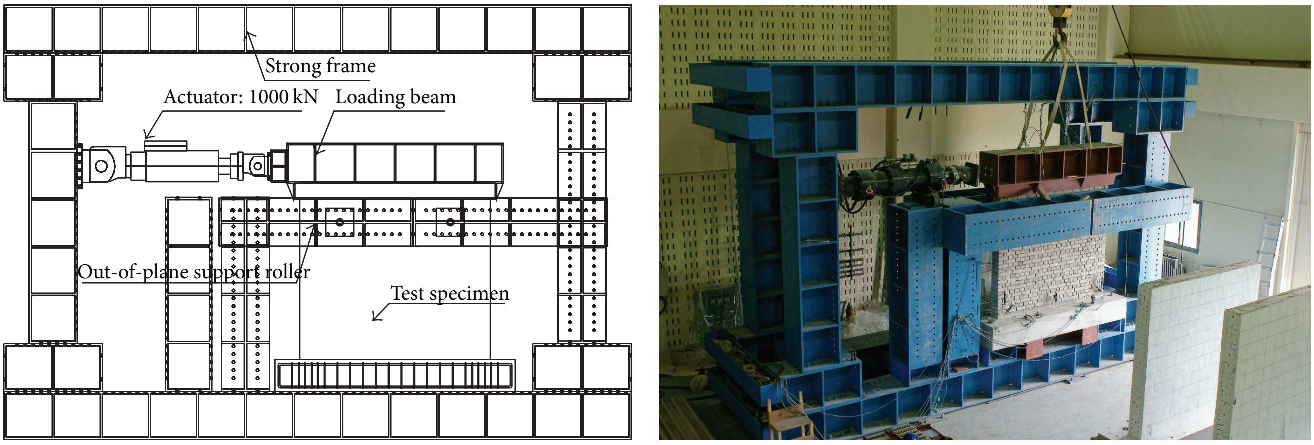

(a)

(b)

Figure 5: Test setup.

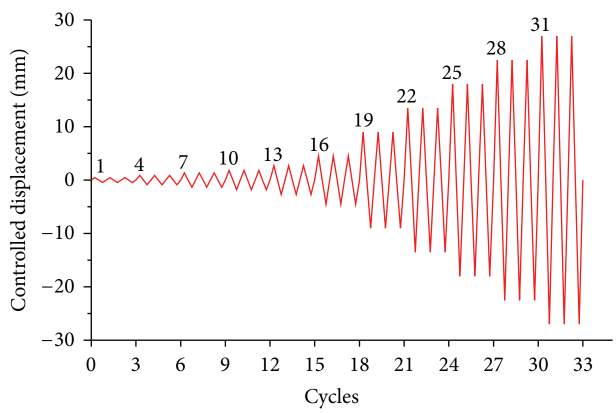

Figure 6: Applied displacement history.

As seen in (3) by Triantafillou [29], there are two different equations to compute effective strain. If each equation is expressed in a graphical way, parabola and straight line shapes are drawn. Then, if the parabola and strain line are connected, a new graph similar to an exponential function is created.

To consider the stress concentration phenomenon and early failure of an FRP sheet, existing experimental data were collected from studies [33–36] where strengthened specimens were similar to the specimens tested in this study. Most of the collected specimens excluding the ones by Calvi and Magenes [33] were strengthened with CFRP and indicated aspect ratios smaller than 1. The effective strain distributions versus strength ratio are depicted in Figure 12. Although the distribution curve is not the same as Triantafillou's in terms of range, its shape presents an exponential function graph as with the model by Triantafillou [29].

Therefore, an equation for URM walls strengthened with FRP composites was derived through nonlinear regression analysis using an exponential function type (5a) and is expressed in (5b). Consider

$$\varepsilon_{\text{eff}} = ae^{(-x/b)} + c, \tag{5a}$$

$$\varepsilon_{\text{eff}} = 0.11683e^{(-\rho_h E_{\text{FRP}}/0.016)} + 0.001. \tag{5b}$$

The test results were compared with the ones estimated using (5b). It was found that the proposed equation was in good agreement with the experimental data by showing a small difference less than 10%. The compared results are provided in Table 6. Relatively less accuracy for the estimation of RTM-CFS-SF was achieved compared to that of RTM-HBRD-SF. As mentioned before, this can be attributed to the fact that RTM-CFS-SF showed early failure by stress concentration of FRP sheet in the vertical direction.

6. Conclusions

In this study, the in-plane behavior of URM walls strengthened with EB FRP sheets was investigated to assess the strengthening effectiveness of FRP sheets on URM walls. Three full-scale masonry wall specimens were examined. The following conclusions can be drawn.

The FRP sheets improved the structural integrity of URM walls. Both CFRP and HFRP were effective in increasing the strength of URM walls by 4.3 and 6 times in comparison with the control specimen.

When FRP composites are used as strengthening materials, debonding and rupture of FRP composites significantly

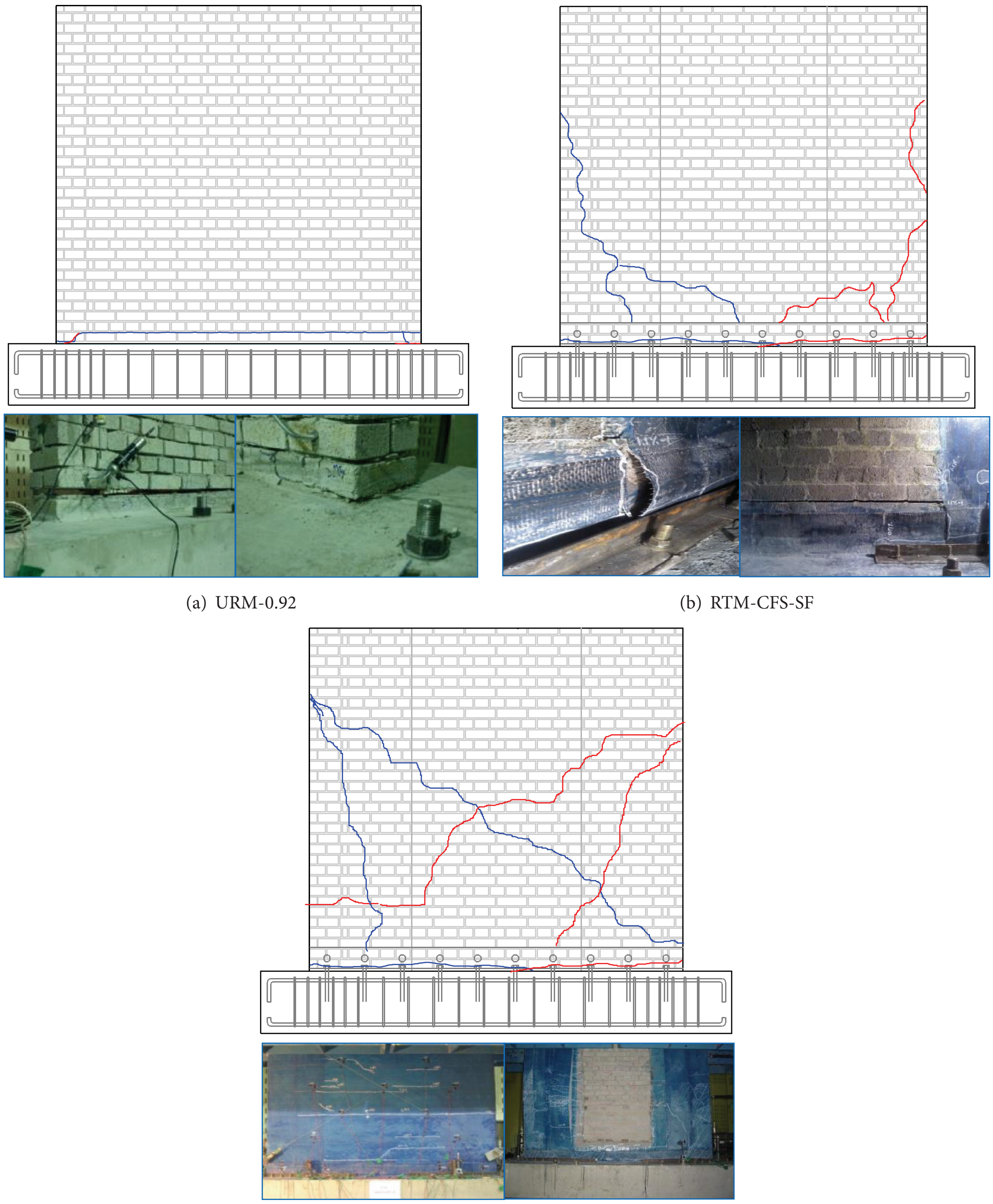

(a) URM-0.92

(b) RTM-CFS-SF

(c) RTM-HBRD-SF

FIGURE 7: Crack pattern and failure mode.

TABLE 6: Evaluation of proposed equation.

Specimen	V_{cal}		V_{test}
	$\varepsilon_{eff,estimate}$	$\varepsilon_{eff,regression}$	
RTM-CFS-SF	518	80	99
RTM-HBRD-SF	308	130	139

affect the lateral resistance of specimens strengthened with FRP materials. Both phenomena occurred in RTM-CFS-SF, resulting in rapid strength decrease. On the contrary, there was no rupture of HFRP in RTM-HBRD-SF, and thus, gradual strength degradation was obtained after the ultimate. Therefore, HFRP consisting of GFRP and AFRP appears to be superior to CFRP from the standpoint of strength and material usage.

The strength of the URM walls strengthened with FRP sheets was estimated using the shear strength model for RC beams by Triantafillou. The accuracy of the model for RC beams was significantly low for the strengthened URM walls since the measured strain of the URM walls retrofitted with

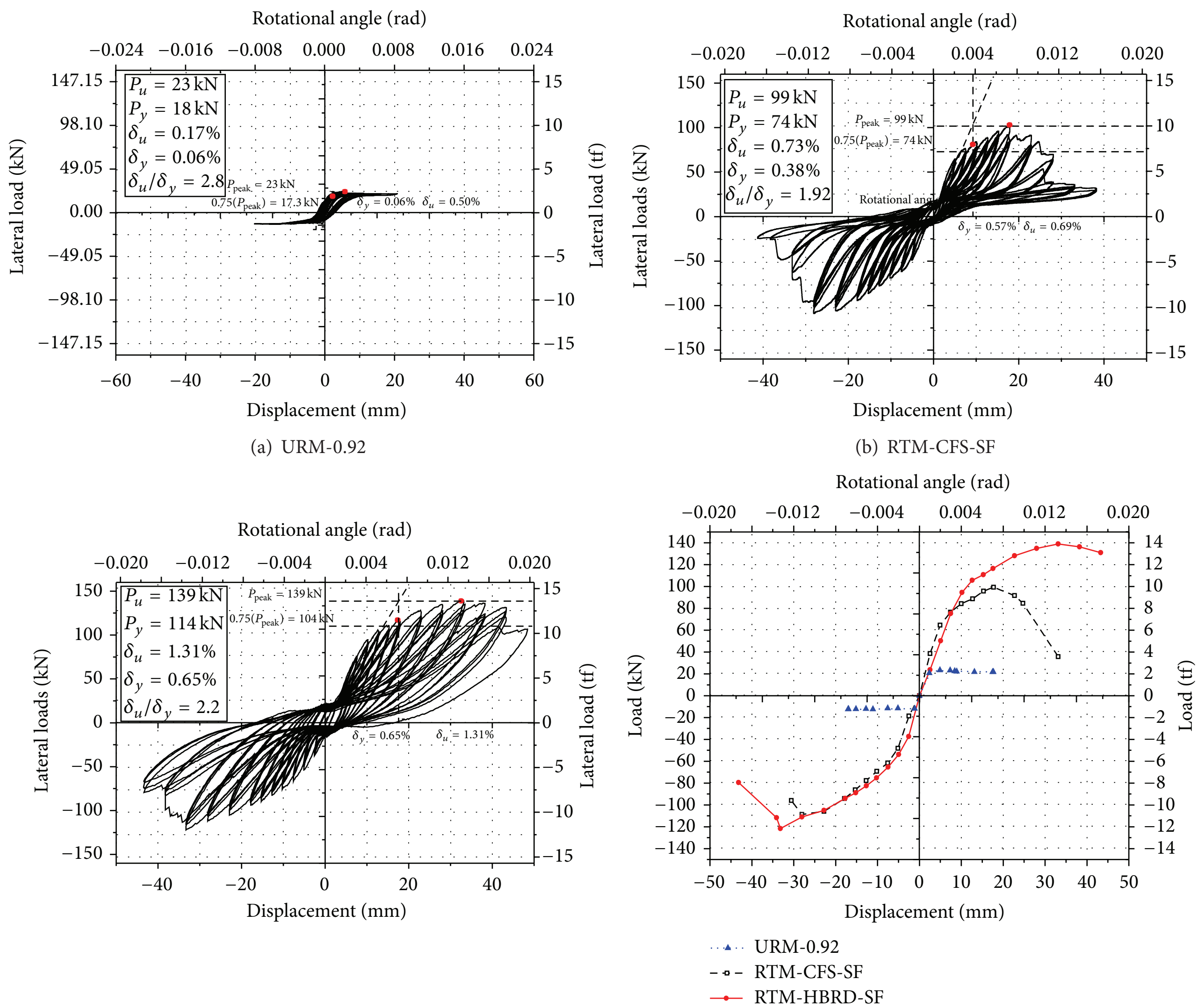

(a) URM-0.92

(b) RTM-CFS-SF

(c) RTM-HBRD-SF

(d) Backbone curve

FIGURE 8: Load-displacement relationship.

FRP sheets was much smaller than that of RC beams used for the shear strength model. Therefore, effective strain is an essential variable for the design of URM walls strengthened with FRP sheet.

An equation is, herein, proposed to estimate an accurate effective strain and consequently the shear strength of URM walls retrofitted with FRP sheet. The suggested model was in good agreement with the test results by indicating a small difference less than 10%. However, it should be noted that the proposed model needs to be applied with care since the number of data used to derive the equation is insufficient.

Notations

A_{FRP}: The cross-sectional area of FRP
A_n: The bonding area of mortar
E_{FRP}: The elastic modulus of FRP
F_{FRP}: The effective strength of FRP material
F_m: The strength of URM walls
f_a: The axial compressive stress (axial compressive force/area of wall)
f_{dt}: The diagonal tension stress
$f_{\mathrm{FRP},u}$: The ultimate tensile strength of FRP sheet
f_j: The axial force of FRP sheet
f'_m: The compressive strength of masonry
h_{eff}: The wall height
L: The wall length
P_E: The expected axial compressive force on wall
Q_{CE}: The shear strength of URM wall
T_g: The glass transition temperature
t: The wall thickness
V_{bjs}: The shear strength in case of bed joint sliding
V_r: The shear strength in case of bed rocking

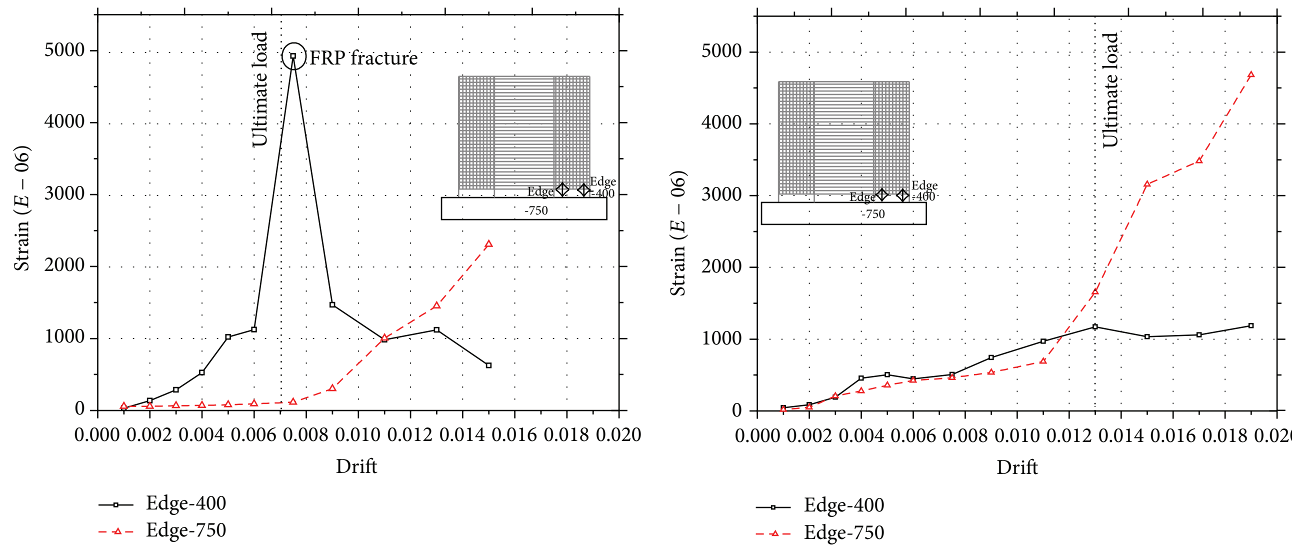

(a) RTM-CFS-SF

(b) RTM-HBRD-SF

Figure 9: FRP sheet strain (vertical direction).

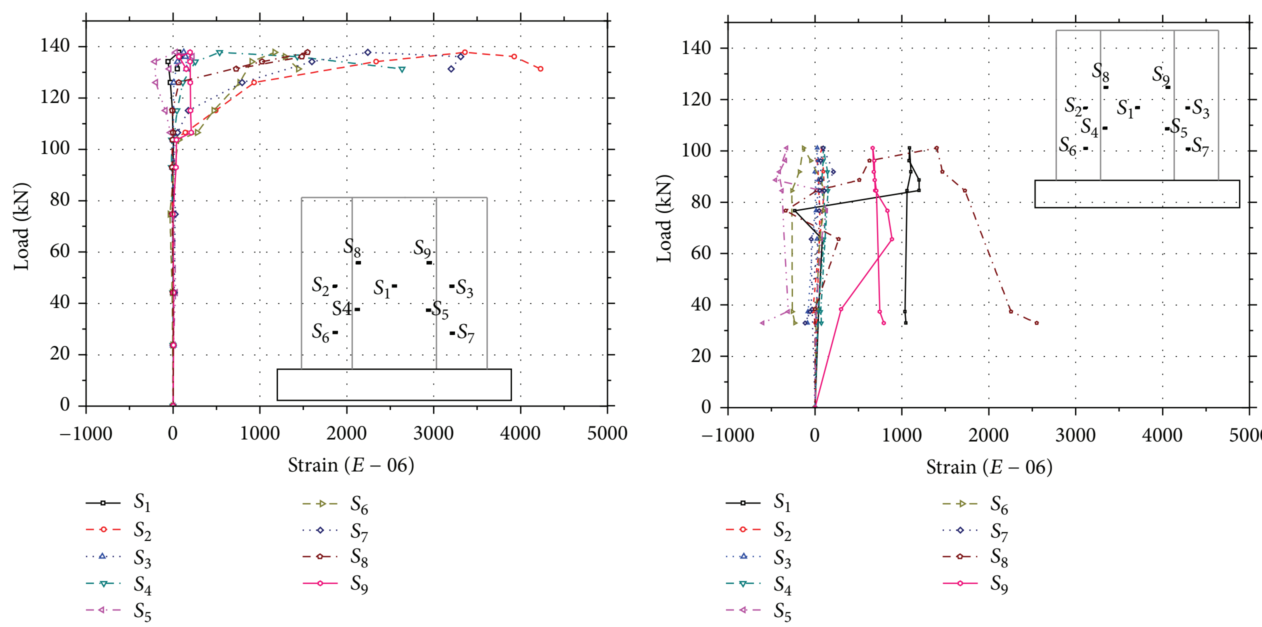

(a) RTM-CFS-SF

(b) RTM-HBRD-SF

Figure 10: FRP sheet strain (horizontal direction).

V_{tc}: The shear strength in case of toe crushing
V_{dt}: The shear strength in case of diagonal tension
v_{me}: The shear stress in case of bed joint sliding
α: The boundary condition constant (0.5 and 1.0 for cantilever and fixed at both ends, resp.)
ε_{eff}: The effective strain of FRP
ρ_h: The strengthening ratio in horizontal direction.

Conflict of Interests

The authors declare that there is no conflict of interests regarding the publication of this paper.

Acknowledgments

This work was supported by Chungwoon University Foundation Grant 2015 and the National Research Foundation of

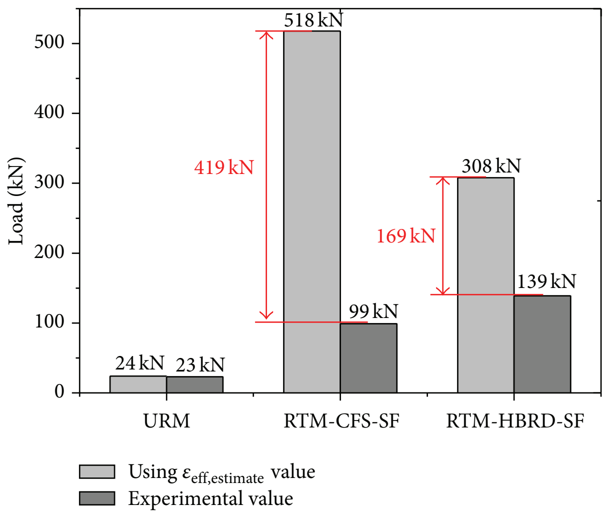

Specimen	$V_{\text{cal,TR98}}$ (kN)	V_{test} (kN)
RTM-CFS-SF	518	99
RTM-HBRD-SF	308	139

FIGURE 11: Evaluation of shear strength.

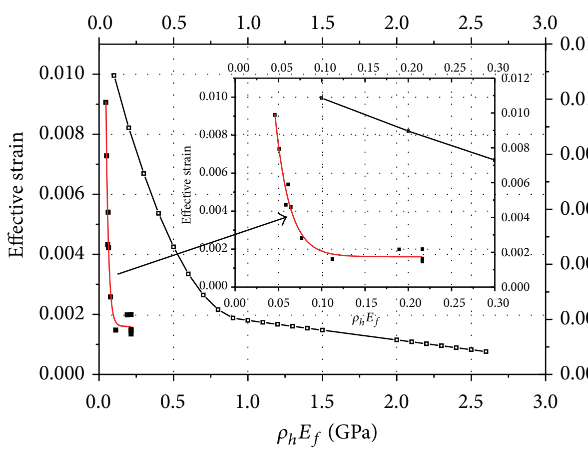

FIGURE 12: Effectiveness strain distribution according to retrofit ratio.

Korea (NRF; 2013R1A1A2010717) grant funded by the Korea government (15CTAP-C097470-01).

References

[1] United States Geological Survey (USGS), http://www.usgs.gov/.

[2] Korea Meteorological Administration (KMA), http://www.kma.go.kr/.

[3] B. C. Park, J. H. Lee, H. Y. Kim, and J. S. Kim, *Study on Seismic Retrofitting Techniques for Unreinforced Masonry Buildings*, Disaster Prevention Research Department, National Disaster Management Institute (NDMI), 2009.

[4] K. Y. Kwan, *Seismic Retrofitting Method for Unreinforced Masonry Buildings*, Earthquake and Disaster Prevention Research Institute of University of Seoul, 2000.

[5] American Society of Civil Engineers (ASCE), "Prestandard and commentary for the seismic rehabilitation of buildings," Tech. Rep. FEMA-356, American Society of Civil Engineers (ASCE), Washington, DC, USA, 2000.

[6] A. Çavdar, "A study on the effects of high temperature on mechanical properties of fiber reinforced cementitious composites," *Composites, Part B: Engineering*, vol. 43, no. 5, pp. 2452–2463, 2012.

[7] A. G. Gibson, M. E. Otheguy Torres, T. N. A. Browne, S. Feih, and A. P. Mouritz, "High temperature and fire behaviour of continuous glass fibre/polypropylene laminates," *Composites Part A: Applied Science and Manufacturing*, vol. 41, no. 9, pp. 1219–1231, 2010.

[8] S. Hinz, T. Omoori, M. Hojo, and K. Schulte, "Damage characterisation of fibre metal laminates under interlaminar shear load," *Composites Part A: Applied Science and Manufacturing*, vol. 40, no. 6-7, pp. 925–931, 2009.

[9] W. Ningyun and J. T. Evans, "Collapse of continuous fibre composite beams at elevated temperatures," *Composites*, vol. 26, no. 1, pp. 56–61, 1995.

[10] S. Kumahara, Y. Masuda, and Y. Tanano, "Tensile strength of continuous fiber bar under high temperature," in *Proceedings of the International Symposium on Fiber-Reinforced Plastic Reinforcement for Concrete Structures*, A. Nanni and C. W. Dolan, Eds., SP-138, pp. 731–742, American Concrete Institute, Farmington Hills, Mich, USA, 1993.

[11] G. L. Balazs and A. Borosnyoi, "Long-term behavior of FRP," in *Proceedings of the International Workshop on Composites in Construction: A Reality*, pp. 84–91, American Society of Civil Engineers, Capri, Italy, July 2001.

[12] J. A. M. Ferreira, J. D. M. Costa, P. N. B. Reis, and M. O. W. Richardson, "Analysis of fatigue and damage in glass-fibre-reinforced polypropylene composite materials," *Composites Science and Technology*, vol. 59, no. 10, pp. 1461–1467, 1999.

[13] C. T. Sun and W. S. Chan, "Frequency effect on the fatigue life of a laminated composite. Composite materials: testing and design (fifth conference)," ASTM STP 674, ASTM International, West Conshohocken, Pa, USA, 1979.

[14] W. Wu, *Thermomechanical properties of fiber reinforced plastics (FRP) bars [Ph.D. thesis]*, West Virginia University, Morgantown, WVa, USA, 1990.

[15] G. Marcari, G. Manfredi, A. Prota, and M. Pecce, "In-plane shear performance of masonry panels strengthened with FRP," *Composites Part B: Engineering*, vol. 38, no. 7-8, pp. 887–901, 2007.

[16] H. S. Maria, P. Alcaino, and C. Luders, "Experimental response of masonry walls externally reinforced with carbon fiber fabrics," in *Proceedings of the 8th U.S. National Conference on Earthquake Engineering*, pp. 8555–8564, San Francisco, Calif, USA, April 2006.

[17] M. R. Valluzzi, D. Tinazzi, and C. Modena, "Shear behavior of masonry panels strengthened by FRP laminates," *Construction and Building Materials*, vol. 16, no. 7, pp. 409–416, 2002.

[18] G. Schwegler, "Masonry construction strengthened with fiber composites in seismically endangered zones," in *Proceedings of*

the 10th European Conference on Earthquake Engineering, pp. 2299–2303, Rotterdam, The Netherlands, 1995.

[19] J. Gergely and D. T. Young, "Masonry wall retrofitted with CFRP materials," in *Proceedings of the Composites in Construction*, J. Figueiras, L. Juvandes, and R. Furia, Eds., pp. 565–569, Porto, Portugal, July 2001.

[20] M. A. ElGawady, P. Lestuzzi, and M. Badoux, "Shear strength of URM walls retrofitted using FRP," *Engineering Structures*, vol. 28, no. 12, pp. 1658–1670, 2006.

[21] M. A. ElGawady, P. Lestuzzi, and M. Badoux, "Aseismic retrofitting of unreinforced masonry walls using FRP," *Composites Part B: Engineering*, vol. 37, no. 2-3, pp. 148–162, 2005.

[22] N. Gattesco and I. Boem, "Experimental and analytical study to evaluate the effectiveness of an in-plane reinforcement for masonry walls using GFRP meshes," *Construction and Building Materials*, vol. 88, pp. 94–104, 2015.

[23] M. El-Diasity, H. Okail, O. Kamal, and M. Said, "Structural performance of confined masonry walls retrofitted using ferrocement and GFRP under in-plane cyclic loading," *Engineering Structures*, vol. 94, pp. 54–69, 2015.

[24] D. Zhou, Z. Lei, and J. Wang, "In-plane behavior of seismically damaged masonry walls repaired with external BFRP," *Composite Structures*, vol. 102, pp. 9–19, 2013.

[25] Y. C. Choi, H. K. Choi, M. S. Lee, and C. S. Choi, "A study on retrofit method of shear wall by new openings," *Magazine of Concrete Research*, vol. 64, no. 5, pp. 377–394, 2012.

[26] S. Ogihara, N. Takeda, S. Kobayashi, and A. Kobayashi, "Effects of stacking sequence on microscopic fatigue damage development in quasi-isotropic CFRP laminates with interlaminar-toughened layers," *Composites Science and Technology*, vol. 59, no. 9, pp. 1387–1398, 1999.

[27] A. Buxton and C. Baillie, "A study of the influence of the environment on the measurement of interfacial properties of carbon fibre/epoxy resin composites," *Composites*, vol. 25, no. 7, pp. 604–608, 1994.

[28] M. A. ElGawady, *Seismic in-plane behavior of URM walls upgraded with composites [Ph.D. dissertation]*, École Polytechnique Fédérale de Lausanne, 2004.

[29] T. C. Triantafillou, "Strengthening of masonry structures using epoxy-bonded FRP laminates," *Journal of Composites for Construction*, vol. 2, no. 2, pp. 96–104, 1998.

[30] AC 125, "Acceptance criteria for concrete and reinforced and unreinforced masonry strengthened using fiber-reinforced polymers (FRP), composite systems," in *Proceedings of the International Conference of Building Officials (ICBO '01)*, Evaluation Service, Whittier, Calif, USA, 2001.

[31] KS F 4004, *Concrete Bricks*, Korea Standards Information Centre, Kyounggi, South Korea, 2013.

[32] ACI 318, "Building code requirements for reinforced concrete," ACI 318-08, American Concrete Institute (ACI) Committee, Farmington Hills, Mich, USA, 2008.

[33] G. Calvi and G. Magenes, "Experimental results on unreinforced masonry shear walls damaged and repaired," in *Proceedings of the 10th International Brick and Block Masonry Conference (IB2MaC '94)*, Calgary, Canada, July 1994.

[34] M. A. ElGawady, P. Lestuzzi, and M. Badoux, "A review of retrofitting of unreinforceed masonry walls using composites," in *Proceedings of the 13th IB2MC*, Paper no. 90, p. 10, Amsterdam, The Netherlands, 2004.

[35] H. Santa-Maria, P. Alcaino, and C. Luders, "Experimental response of masonry walls externally reinforced with carbon fiber fabrics," in *Proceedings of the 8th U.S. National Conference on Earthquake Engineering*, San Francisco, Calif, USA, 2006.

[36] M. Seki, R. Vacareanuu, T. Saito et al., "Cyclic shear tests on plain and FRP retrofitted masonry walls," in *Proceedings of the 14th World Conference on Earthquake Engineering*, Beijing, China, October 2008.